Solution Processed of Solid State HTL of CuSCN Layer at Low Annealing Temperature for Emerging Solar Cell

O. V. Aliyaselvam*, F. Arith*‡, A. N. Mustafa** M. K. Nor** Oras Ahmed Al-Ani***

*Centre for Telecommunication Research & Innovation, Faculty of Electronic and Computer Engineering, Universiti Teknikal Malaysia Melaka, Malaysia.
**Centre for Telecommunication Research & Innovation, Faculty of Electrical and Electronic Engineering Technology, Universiti Teknikal Malaysia Melaka, Malaysia

***Electrical Engineering Technical College, Middle Technical University, Baghdad, Iraq.

Corresponding Author; Faiz Arith, Centre for Telecommunication Research & Innovation, Faculty of Electronic and Computer Engineering, Universiti Teknikal Malaysia Melaka, Malaysia
Tel: +60 10-355 7758, E-mail: faiz.arith@utem.edu.my

Received: 12.05.2021 Accepted:07.06.2021

Abstract- High density and uniform Hole Transport Layer (HTL) Copper (I) thiocyanate (CuSCN) was prepared directly on Indium-doped Tin Oxide (ITO) substrate through two-step spin coating technique and followed by low temperature annealing process. A new solvent of Monoethanolamine (MEA) with no additive was introduced for the preparation and yet producing a comparable result of HTL for perovskite solar cell application. The CuSCN layer was characterized for its surface morphology, crystallinity and optical features by using Scanning Electron Microscope (SEM), X-Ray Diffraction (XRD) and Ultraviolet-Visible Spectroscopy (UV-Vis) respectively. Furthermore, the resistivity of the layer was also measured by I-V measurement. An optimized annealing temperature of 100 °C is obtained, resulting pristine morphology structure and high conductivity of 77.30 S/m. This paper is the first to report the use of MEA as a solvent for CuSCN layer, showing that the right combination of solvent use and annealing temperature can produce a good CuSCN structure. Thus, being able to produce HTL layers more easily, rapid and at minimal cost, in turn having a positive impact in reducing the cost of solar cell production.

Keywords: CuSCN, Hole Transporting Layer, MEA, Spin-coating

1. Introduction

New emerging solar cell technology is currently advancing over the decade and accomplishes good efficiency, specifically dye-sensitized solar cells (DSSCs) and perovskite solar cells (PSCs) [1]. However, liquid electrolytes employed as a hole transport layer (HTL) or light absorber in new emerging solar cell applications have a crucial drawback as it degrades the device stability due to evaporation of liquid caused by heat and even encounters practical issues like liquid contamination and leakage [2, 3]. Therefore, solid-state hole transport material is a promising alternative for

liquid-electrolytes in a solar cell structure to sustain its stability and efficiency [4–8].

The increasing number of photovoltaic studies is currently focused on finding a promising material to employ as the inter HTL system. A handful of p-type semiconductors are appropriate to act as hole transport material in solar cell applications, such as silicon carbide (SiC), gallium nitride (GaN), and 2,2′-7,7′-tetrakis (N,N-di-p-methoxyphenyl-amine) 9,9′-spirobifluorene (spiro-OMeTAD) and poly(3,4-ethylenedioxythiophene):polystyrene sulfonate (PEDOT: PSS) [9–14]. Yet, both SiC and GaN require high processing temperatures for their deposition and damage the other operating layers of a solar cell. Although spiro-OMeTAD provides high hole mobility, it is overpriced and also causes excessive interfacial of hole and electron, resulting recombination losses and affecting cell stability in the long term [15]. Meanwhile, recent studies state that due to acidic nature and semi-metallic nature, PEDOT: PSS, reacts with organically active layers and underlying transparent ITO electrode, which limits the long-term operational stability and provides insufficient electron blocking properties, respectively [16].

Nevertheless, the copper-based material with a wide-bandgap, namely copper(I) thiocyanate (CuSCN) shows good characteristics and conductivity to perform as HTL through a simple deposition method at the optimized condition [6, 17]. CuSCN is a transparent solid wide-bandgap p-type semiconductor and has various emerging applications for optoelectronic and photovoltaic applications as solid hole-transporting electrolytes in DSSCs and PSCs [18–20]. Initially, CuSCN was first used as HTL by Fernando *et al.* [5] in 1994 and reported to have higher photocurrent quantum efficiency compared to the conventional photo-electrochemical cells. Smith *et al.* [21] compared the hexagonal crystal structure's atomic parameters and concluded that smaller hexagonal crystals seemed to have better quality. On the contrary, Yong Ni *et al.* [19] summarized that larger grain-sized CuSCN performed well at its optimum temperature and exhibited high-level transmittance (>87%) in the visible wavelength range with a direct bandgap of 3.88 eV. It is also mentioned that there are several aspects like copper vacancies, applied potentials, electrolyte components, and deposition temperatures that are capable of influencing the particle morphology, the band structure of CuSCN [22, 23]. The following research by P. Pattanasattayavong *et al.* [24] insisted that further improvements can be made on CuSCN by performing an effective p-type doping method to have a broader band gap hole-transporting semiconductor with many promising electronic characteristics. Conclusively, despite optimizing the hole-transport characteristics of CuSCN theoretically, other factors have a positive influence on its band structure, intrinsic and electronic and optical properties.

Various deposition techniques have been employed in depositing CuSCN as HTL, such as spin coating, screen printing, spray coating, doctor blading and electrodeposition which contribute well for commercialization purpose [21, 22]. Lv *et al*. [27] experimented on fully air-processed PSC stability using CuSCN as HTL and conquered PCE of 10.01%. The fabrication of CuSCN-based PSC via spin-coating technique by Arora *et al*. [28] achieved 20.4% of PCE. Similarly, Jung *et al*. and Yaacobi-Gross *et al.* [16, 29] also implemented the spin-coating technique to deposit the CuSCN layer and achieved 10.3% and 6.5% of PCE, respectively. By performing a simple spray deposition technique, a highly uniform and crystallized CuSCN layer with a thickness of ~50 nm is produced with a PCE of 17%.

The effect of thermal annealing of CuSCN on photovoltaic performance is crucial as it is linked to charge carrier mobility [30, 31]. F. Matebese *et al.* [32] proved that annealing has a significant impact on solar cell efficiency as his research outcome exhibited different photovoltaic performances for different annealing temperatures. Jung *et al*. [29]

reported the PCE_{MAX} can be further increased to 16% after thermal annealed at 100 °C. Conversely, thermal annealing beyond 100 °C weakens the device's performance. However, A. Nizamuddin *et al.* [33] concluded based on his SEM images observation that CuSCN particles started to dissolve when annealed at 90 °C and beyond. Therefore, optimization of annealing temperature is vital to achieving good photovoltaic efficiency as it enhances CuSCN's charge carrier mobility.

Several comparative studies among HTLs have proved that device performance and long-term stability are strongly dependent on the hole-transporting material. According to Tiep *et al*. [7] some factors diminish the devices' stability, such as temperature, UV radiation, and structural changes during the working operation. Based on a study by Yaacobi-Gross *et al*. [16], he concluded that CuSCN exhibited a bulk heterojunction cell with both polymer and small molecule as an active layer material system efficiently, thereby elevated the J_{SC} while maintaining high V_{OC} and FF, increasing the CuSCN-based solar cell's PCE_{MAX} to ≈ 6.5%. Likewise, the research outcome by Yaacobi-Gross *et al*. is much supported by Kim *et al.* [34] in his investigation as he concluded that CuSCN has the potential to substitute PEDOT: PSS due to its high optical transparency, high hole mobility, better exciton blocking ability, and good chemical stability, thus provides good hole conductivity. Besides, Chaudhary *et al.* [6] emphasized applying eco-friendly and inexpensive solvent for solution-processable deposition of CuSCN as an efficient HTL with PCE achieved up to 4.2%. To sum up, CuSCN-based solar cells shows better long-term environmental and thermal stability in ambient conditions than other HTL-based PSC [7, 35, 36].

In this study, the research aims to innovate a simple low-cost fabrication method of CuSCN as HTL with optimized annealing condition at a low temperature (<150 °C) without the use of additional additives or conventional solvent like acetonitrile.

2. Methodology

2.1 Deposition of CuSCN

As for the preparation of the substrate, ITO glass is soaked in an ethanol-filled beaker, CuSCN solution. Then, the CuSCN solution again put in the ultrasonic bath at 70 °C until the desired solution is formed.

The following step covered with aluminium foil and put in an ultrasonic cleaner at 70 °C for 10 min to eliminate unwanted contamination of the substrate. Then, the substrate is dried on a hot plate at 100 °C for 10 min. Then, the 3 ml of ethanol is added to 200 mg of CuSCN powder. Once covering the beaker tightly with aluminium foil, the mixed CuSCN solution is immersed in the ultrasonic bath at 70 °C for 10 min, to dilute the solution. After 20 h, three drops of monoethanolamine (MEA) is added to the is to deposit the CuSCN solution onto the ITO glass by performing a two-step spin-coating technique. The CuSCN solution is dripped onto the ITO glass substrate for each sample until 75% of its covers. Then, the sample is spin-coated twice with a two-step process. The first spin-coating is used to produce a uniformly planar surface, while the latter step is to deposit desired thin layer on ITO glass. The first two-step process involved with spins is different in speed, namely 500 rpm for 5 s, and 800 rpm for 30 s. Next, the second two-step process is spun at 500 rpm for 5 s, 2800 rpm for 30 s. Finally, the annealing temperature for each CuSCN sample is varied from 80 °C to 120 °C, thereby the process is carried out on a hot plate for 70 min.

2.2 Characterization

Zeiss EVO 18, Scanning electron microscopy (SEM) is used to characterize the layer surface morphology features and particle growth density. Besides, the PANalytical X'Pert Pro X-ray diffraction (XRD) is used to identify the deposited layers' crystal structure. Shimadzu UV-1800/Visible Scanning Spectrophotometer has performed

ultraviolet-visible spectroscopy to demonstrate absorbance, transmittance, and bandgap of the CuSCN layer.

3. Results, Analysis and Discussion

3.1 Structural performance of CuSCN

The SEM images of CuSCN samples annealed at different temperatures are shown in Figure 1. The images are magnified at ~100 times magnification for crystal structure identification of CuSCN annealed on ITO glass. As shown in Figure 1 (a), the CuSCN sample structure annealed at 80 °C is not mesoporous. Hence, it appeared less dense. Despite being less dense, the CuSCN sample annealed at 90 °C has observed that the solvent mixed in the deposited solution is not fully evaporated during the annealing process, as shown in Figure 1 (b). Meanwhile, high density of the crystalline growth in all three CuSCN samples annealed at 100 °C, 110 °C, and 120 °C, are demonstrated in Figure 1 (c), (d), and (e), respectively.

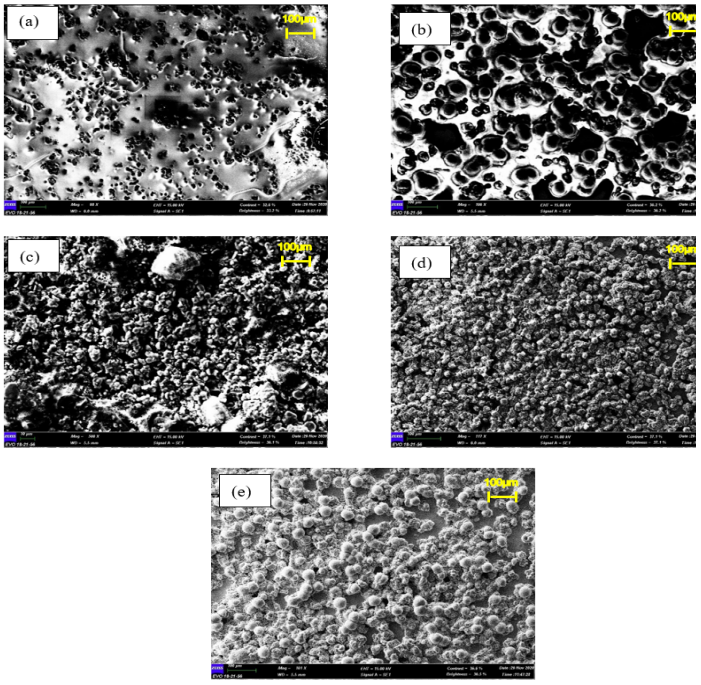

Fig. 1. SEM images; top view of CuSCN annealed at different temperatures at ~100 times magnification, a) 80 °C, (b) 90 °C, (c) 100 °C, (d) 110 °C, and (e) 120 °C

The particles of CuSCN annealed at 100 °C at 2000 times magnification in Figure 2 clearly shows that demonstrates high density and uniformity in grain growth with an average grain diameter of 5.32 µm. Nevertheless, CuSCN grains annealed at 120 °C observed to have the worst outcome with destructed grain structures. Although the particles' uniformity demonstrates high mesoporous, the grain appeared broken, as shown in Figure 3. This can be interpreted as the CuSCN particles enact melting behaviour during the annealing process at 120 °C due to high temperature [21]. Similarly, Jung *et al*. [27] also reported that thermal annealing beyond 100 °C degrades the photovoltaic properties of the cell due to changes in the charge carrier mobility of CuSCN. Inevitably, the particles travel quickly in all directions but collide more often in a solid state than in a liquid due to shorter distances between particles. Therefore, a proper annealing condition can mitigate the internal crystalline structure imperfections while improving the charge carrier transportation, yet with an increase in temperature, the particles travel faster as they accumulate kinetic energy, resulting in increased collision rates [29, 37].

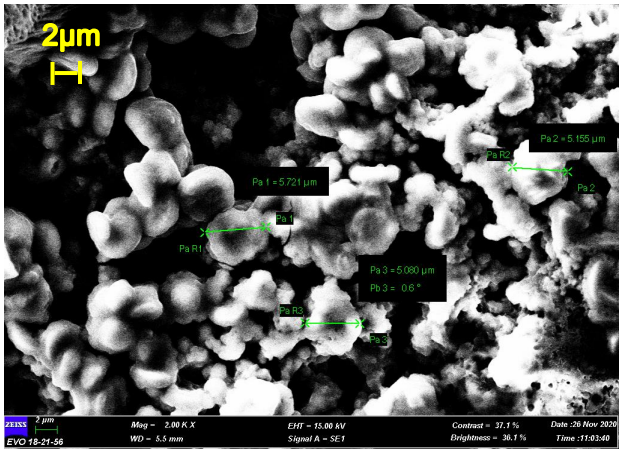

Fig. 1. SEM image; top view of CuSCN annealed at 100 °C at 2000 times magnification

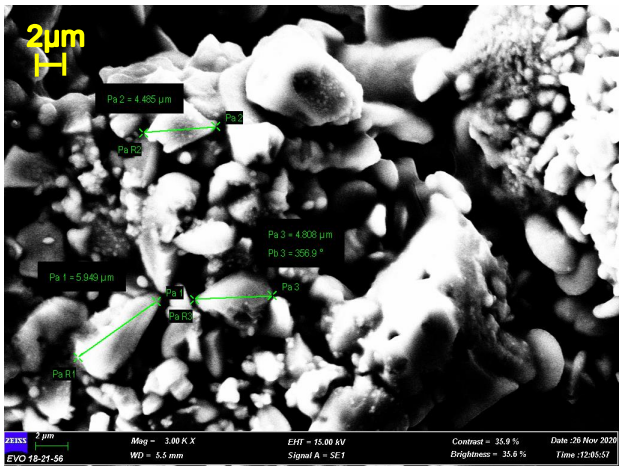

Fig. 3. SEM image; top view of CuSCN annealed at 120 °C at 3000 times magnification

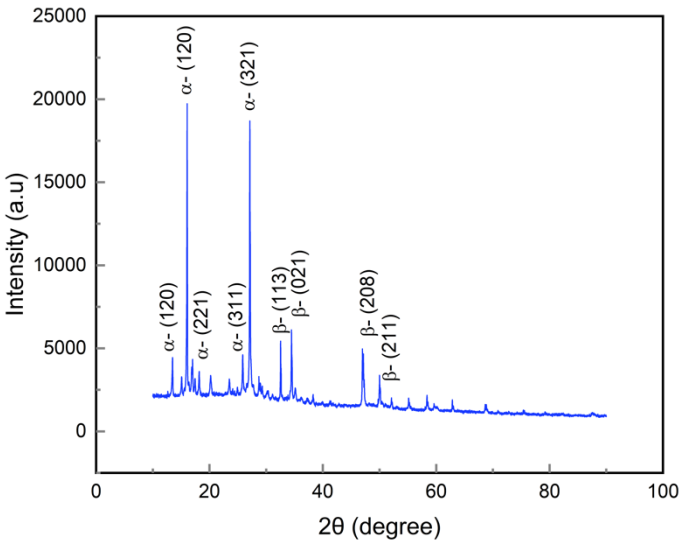

Fig. 4. XRD pattern of deposited CuSCN layer

XRD pattern in Figure 4, is used to examine the crystalline structure and the presence of CuSCN material on its substrate. The diffraction peaks of CuSCN can be classified into two different formations of phase, which are orthorhombic and rhombohedral phase or call it as α-CuSCN and β-CuSCN. The CuSCN layer which annealed at 100 °C has distinct, and strong peaks observed at 13.1°, 15.8°, 25.9°, 27.1°, and 27.6° which corresponds to the (120), (200), (221), (311), and (321) planes of orthorhombic α-CuSCN phase, matched with single standard JCPDS data (00-029-0582). Moreover, the intense diffraction peaks at 31.9°, 35.0°, 45.4°, and 46.8° are corresponding to (113), (021), (208), and (211) planes of the rhombohedral β-CuSCN phase as referred to standard JCPDS data (00-029-0581). CuSCN is a semiconductor material that possesses a wide bandgap and thereby assumed to have few native defects in the gap, especially in β-CuSCN as it has the lowest band transition [22, 38]. Therefore, the sharp peaks of α-CuSCN, defines that there is a substantial amount of intrinsic defects.

3.2 Optical performance of CuSCN

The optical performance of CuSCN is analyzed by demonstrating UV-Vis of the deposited CuSCN layers annealed at different temperatures, ranging between 80 °C to 120 °C. The wavelength for both absorbance and transmittance is taken at the range electromagnetic spectrum. Figure 5 presents the absorption of each layer where the amount of incident light energy reflected and absorbed at each deposited layer at various wavelengths. All the CuSCN samples attained their highest absorbance level when the wavelength is at 339.5 nm.

Conversely, the plotted transmittance curve of CuSCN samples at different annealing temperatures in Figure 6 shows that all the CuSCN samples have a distinctly higher level of transmittance from 85% to 91%, with a peak of 339.5 nm. As an outcome, the deposited CuSCN layers' transmittance plot dropped drastically in the range of 34% to 45%, and it occurred may be due to an increase of scattered light at the particle growth density. This is because the thickness and uniformity of a CuSCN layer dominate the light scattering effects, and further interferes with the inter-planar spacing between the atoms and stacking faults [39–41]. Indeed, when the absorbance is high, the transmittance is low since these two fundamentally contradict each other. Hence, CuSCN as HTL is capable of optic and photovoltaic applications due to high transparency and direct absorption measurements.

By having an absorption and transmission curve, optical bandgap energy can be ascertained. The theory of optical absorption interrelates the absorption coefficient and the photon energy, for direct allowed transition as Equation (1) below.

$$\alpha hv = A(hv - Eg)^{\frac{1}{2}} \quad (1)$$

The plot of the absorption coefficient (αhv^2) against the photon energy (hv) for CuSCN films annealed at a different temperature is showed in Figure 7, where α defined as the absorption coefficient, h is Planck's constant of 1240 eV-nm, while v and Eg is the light frequency and bandgap, respectively. According to semiconductor physics, n has a value of 2 for direct bandgap semiconductors. Moreover, the absorption coefficient (α) is obtained by having the absorbance value over the deposited film's thickness, 50 nm.

In this study, αhv^2 against hv provides good linearity, and henceforth all the CuSCN have a direct band transition shown in Figure 7. CuSCN films deposited and characterized via different techniques result in energies ranging from 3.6 eV to 3.94 eV, as often cited in research work [42, 43]. However, CuSCN annealed at 90 °C deposited via spin-coating technique attained the highest bandgap energy, which is 2.53 eV, yet much smaller than the reported bandgap. Likewise, Ezealigo *et al*. [44] documented a similar range of bandgap values in their research. In this context, the decrease in the bandgap of CuSCN layers may be due to the deposition technique or condition that causes improvement in the films' crystalline quality and the increase of particle size as the temperature increases [45, 46].

3.3 Electrical performance of CuSCN

I-V characteristics are performed for each CuSCN sample for electrical characterization. Current is measured by varying bias voltages ranging from 0.5 V to 5 V as the power supply supplied the voltage, while the ITO coated glass, CuSCN substrates, and the measurement setup is connected serially. The current is then determined by connecting the measurement setup in series to a negative probe of

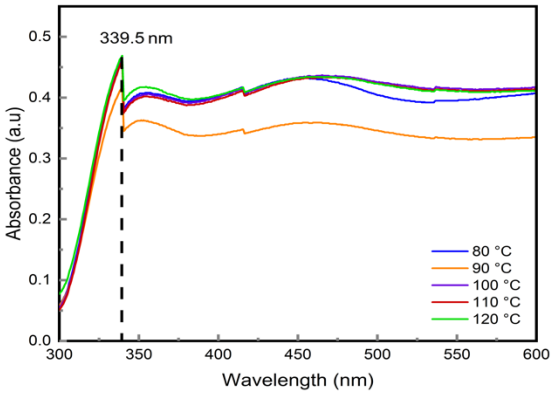

Fig. 5. Absorbance curve of CuSCN samples annealed at different temperatures, ranges between 80 °C to 120 °C

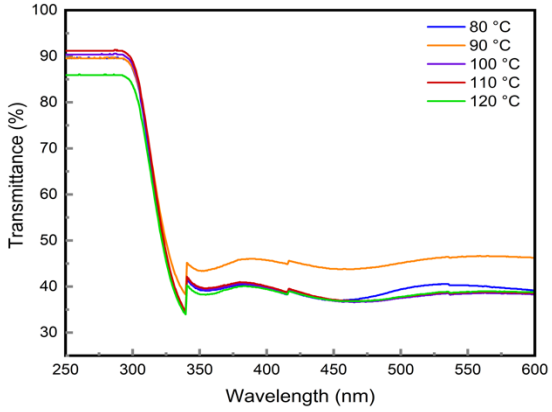

Fig. 6. Transmittance curve of CuSCN samples annealed at different temperature, ranges between 80 °C to 120 °C

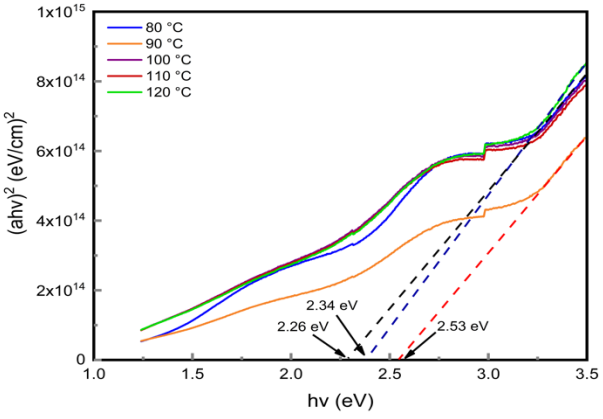

Fig. 7. Bandgap curve of CuSCN samples annealed at different temperatures, ranges between 80 °C to 120 °C

power supply, and another probe is connected to the substrate. At the same time, the positive probe of the power supply is connected to the substrate.

The measured current is increased with the increase in the applied voltage, whereby each line is directly proportional as illustrated in Figure 8. As charted in Figure 9, the conductivity against each annealing temperature of CuSCN samples is plotted by obtaining the gradient from the graph in Figure 8. Moreover, the CuSCN substrate annealed at 100 °C showed the highest and outstanding conductivity of 77.3 S/m in the conductivity versus temperature graph. Besides, the substrate annealed at 90 °C is the second high of conductivity, then followed by other temperatures in a sequence of 80 °C and 120 °C. Surprisingly, samples annealed at 100 °C and 110 °C have shown the same gradient value and, thus, conductivity. Essentially, the conductivity of a material is greatly dependent on applied voltages, whereas grain boundaries in nanocrystalline materials often have a direct impact on the flow of electronic current [47, 48]. Conclusively, the CuSCN sample is suggested to anneal at 100 °C as it offers the best electrical efficiency compared to other samples.

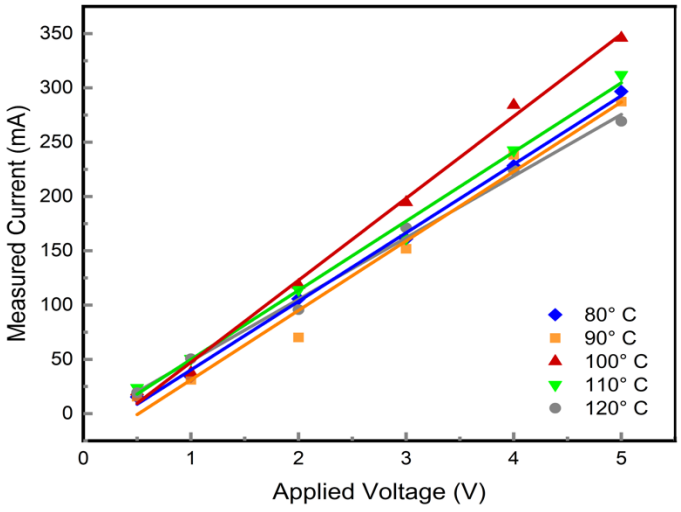

Fig. 8. I-V characteristics for CuSCN samples annealed at different temperatures, ranges from 80 °C to 120 °C

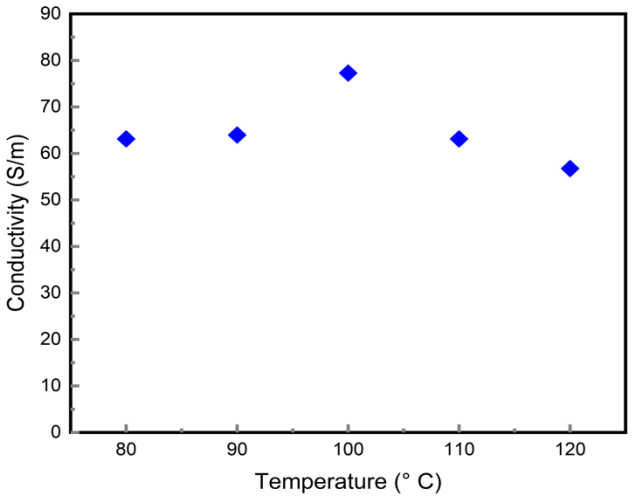

Fig. 9. Conductivity of CuSCN layers at different annealing temperatures

The CuSCN films deposited through several conventional methods are tabulated in Table 1. Method 1 demonstrates electrodeposition of CuSCN films through new (TEA, N(CH2CH2OH)3)-chelated aqueous electrolytes with weak basic, while propyl sulfide and fused quartz are used as solvent and substrate, respectively for spin-coating in Method 2. Additionally, Method 3 comprises SILAR cycle with various chemicals used for CuSCN deposition, such as copper sulphate pentahydrate ($CuSO_4 \cdot 5H_2O$), sodium thiosulphate ($Na_2S_2O_3 \cdot 5H_2O$), sodium thiocyanate (NaSCN), sodium sulphate (Na_2SO_4), and sodium thiosulphate ($Na_2S_2O_3$).

Conversely, the resulting parameters for each method in Table 1 have shown parallel results as conducted in this research by creating a simple method with unprecedented solvent, namely monoethanolamine (MEA), thus minimizing the fabrication cost. Inevitably, it is shown clearly that the trailblazing in this work has demonstrated sufficient properties of CuSCN to act as solid-state HTL in solar cell applications, with a minimal-costed fabrication.

Table 1. Comparison table of CuSCN layers using different methods.

Method	Bandgap (eV)	Absorbance (nm)	Transmittance (%)
1	3.88	320	>87
2	3.90	290	>70
3	2.85	350	NA
Our work	2.35	339.5	>91

Conclusion

HTL as light-absorbing material in solar cell applications, such as PSC and SSDSSC can influence the performance of the cell in term of stability and reliability. Therefore, CuSCN as p-type semiconducting HTL is introduced to replace the conventional HTL, namely spiro-OMeTAD and PEDOT:PSS. Besides, CuSCN is successfully deposited on the ITO substrate by performing a two-step spin-coating technique. The speed and duration of spinning are fixed when performing a two-step process. The first spin-coating is used to produce a uniform coating surface, while the second spin-coating is used to produce a thin layer of HTL on ITO glass. Then, the annealing temperature of CuSCN is optimized in the range of 80 °C to 120 °C based on the analysis of structural, optical and electrical characteristics. The structural characteristics are determined by scanning electron microscopy (SEM), and X-ray diffraction (XRD). Meanwhile, the electrical and optical characteristic is measured by I-V characteristics and UV-Vis, respectively. The SEM images of CuSCN at 100 °C showed high dense and particle growth compared with other annealing temperatures. From the I-V characteristics, the CuSCN layer annealed at 100 °C resulted in 77.30 S/m of conductivity. Despite the lack of additives, dopants and high-end solvents, the fabricated CuSCN as HTL has showed promising features to be as HTL under optimized annealing conditions, while minimizing the fabrication costs. In conclusion, the best annealing temperature for CuSCN to perform as HTL in this work is 100 °C.

Acknowledgement

The work of O. V. Aliyaselvam was supported by the Zamalah Scheme, Universiti Teknikal Malaysia Melaka, Malaysia.

References

[1] S. Sharma, K. K. Jain, and A. Sharma, "Solar Cells: In Research and Applications—A Review," *Materials Sciences and Applications*, vol. 06, no. 12, pp. 1145–1155, 2015.

[2] K. Tennakone, G. R. R. A. Kumara, I. R. M. Kottegoda, and V. P. S. Perera, "An efficient dye-sensitized photoelectrochemical solar cell made from oxides of tin and zinc," *Chemical Communications*, no. 1, pp. 15–16, 1999.

[3] Z. Yang, K. C. Powers, D. J. Liu, Y. Ren, and T. Xu, "Solid dye-sensitized solar cells prepared through a counter strategy for filling of solid hole transporter," *Journal of Renewable and Sustainable Energy*, vol. 3, no. 6, 2011.

[4] K. Ranabhat, L. Patrikeev, A. A. evna Revina, K. Andrianov, V. Lapshinsky, and E. Sofronova, "An introduction to solar cell technology," *Journal of Applied Engineering Science*, vol. 14, no. 4, pp. 481–491, 2016.

[5] C. A. N. Fernando, A. Kitagawa, M. Suzuki, K. Takahashi, and T. Komura, "Photoelectrochemical properties of rhodamine-C18 sensitized p-CuSCN photoelectrochemical cell (PEC)," *Solar Energy Materials and Solar Cells*, vol. 33, no. 3, pp. 301–315, 1994.

[6] N. Chaudhary, R. Chaudhary, J. P. Kesari, and A. Patra, "An eco-friendly and inexpensive solvent for solution processable CuSCN as a hole transporting layer in organic solar cells," *Optical Materials*, vol. 69, pp. 367–371, 2017.

[7] N. H. Tiep, Z. Ku, and H. J. Fan, "Recent Advances in Improving the Stability of Perovskite Solar Cells," *Advanced Energy Materials*, vol. 6, no. 3, pp. 1–19, 2016.

[8] W. Tress, N. Marinova, O. Inganas, M. K. Nazeeruddin, S. M. Zakeeruddin, and M. Graetzel, "The role of the hole-transport layer in perovskite solar cells - Reducing recombination and increasing absorption," *2014 IEEE 40th Photovoltaic Specialist Conference, PVSC 2014*, pp. 1563–1566, 2014.

[9] O. Eyecioglu, M. Beken, and O. Icelli, "Effect of Boric

Acid Doped Pedot : PSS Layer on the Photovoltaic Parameters of P3HT : PCBM Based PV," *7th International Conference on Renewable Energy Research and Applications, ICRERA 2018,* vol. 5, pp. 3–5, 2018.

[10] A. L. P. Dilan, "Quantum photovoltaic effect: Two photon process in solar cell," *4th International Conference on Renewable Energy Research and Applications, ICRERA 2015*, vol. 5, no. 1, pp. 1084–1088, 2015.

[11] P. Chelvanathan, S. A. Shahahmadi, F. Arith, K. Sobayel, M. Aktharuzzaman, K. Sopian, F. H.Alharbi, N. Tabet, and N. Amin "Effects of RF magnetron sputtering deposition process parameters on the properties of molybdenum thin films," *Thin Solid Films*, vol. 638, pp. 213–219, 2017.

[12] H. Sun, S. Lin, R. Zhang, K. Yang, M. Xia, W. Li, and W. Guo "Perovskite solar cells employing Al_2O_3 scaffold layers," *3rd International Conference on Renewable Energy Research and Applications, ICRERA 2014*, pp. 442–444, 2014.

[13] J. Goilard, K. Xue, C. Renaud, P. Y. Chen, S.-H. Yang, and T.-P. Nguyen, "Investigations of Defects in Inverted Organic Solar Cells," in *International Conference on Engineering Research and Applications*, *ICRERA 2019*, pp. 448–454, 2019.

[14] A. Parisi, L. Curcio, V. Rocca, S. Stivala, A.C. Cino, C. Alessandro, G. Cipriani, D. L. Cascia, V. D. Dio, R. Miceli, "Photovoltaic module characteristics from CIGS solar cell modelling," *International Conference on Engineering Research and Applications ICRERA 2019,* no. October, pp. 20–23, 2019.

[15] J. E. Kroeze, N. Hirata, L. Schmidt-Mende, C. Orizu, S. D. Ogier, K. Carr, M. Grätzel, and J. R. Durrant, "Parameters influencing charge separation in solid-state dye-sensitized solar cells using novel hole conductors," *Advanced Functional Materials*, vol. 16, no. 14, pp. 1832–1838, 2006.

[16] N. Yaacobi-Gross, N. D Treat, P. Pattanasattayavong, and H .Faber, "High-efficiency organic photovoltaic cells based on the solution-processable hole transporting interlayer copper thiocyanate (CuSCN) as a replacement for PEDOT:PSS," *Advanced Energy Materials*, vol. 5, no. 3, pp. 1–7, 2015.

[17] H. Iftikhar, G. G. Sonai, S. G. Hashmi, A. F. Nogueira, and P. D. Lund, "Progress on electrolytes development in dye-sensitized solar cells, " *Materials,* vol. 12, no. 12. 2019.

[18] L. Calió, S. Kazim, M. Grätzel, and S. Ahmad, "Hole-Transport Materials for Perovskite Solar Cells," *Angewandte Chemie - International Edition*, vol. 55, no. 47, pp. 14522–14545, 2016.

[19] E. L. Ratcliff, B. Zacher, and N. R. Armstrong, "Selective interlayers and contacts in organic photovoltaic cells," *Journal of Physical Chemistry Letters*, vol. 2, no. 11, pp. 1337–1350, 2011.

[20] M. Grätzel, "Dye-sensitized solar cells," *Journal of Photochemistry and Photobiology C: Photochemistry Reviews*, vol. 4, no. 2, pp. 145–153, 2003.

[21] D. L. Smith and V. I. Saunders, "Preparation and structure refinement of the 2H polytype of β-copper(I) thiocyanate," *Acta Crystallographica Section B Structural Crystallography and Crystal Chemistry*, vol. 38, no. 3, pp. 907–909, 1982.

[22] J. E. Jaffe, T. C. Kaspar, T. C. Droubay, T. Varga, M. E. Bowden, and G. J. Exarhos, "Electronic and defect structures of CuSCN," *Journal of Physical Chemistry C*, vol. 114, no. 19, pp. 9111–9117, 2010.

[23] Y. Ni, Z. Jin, and Y. Fu, "Electrodeposition of p-type CuSCN thin films by a new aqueous electrolyte with triethanolamine chelation," *Journal of the American Ceramic Society*, vol. 90, no. 9, pp. 2966–2973, 2007.

[24] P. Pattanasattayavong, O. N. Ndjawa, K. Zhao, K. Wei Chou, N. Yaacobi-Gross, B. C. O'Regan, A. Amassianb and T. D. Anthopoulos, "Electric field-induced hole transport in copper(I) thiocyanate (CuSCN) thin-films processed from solution at room temperature," *Chemical Communications*, vol. 49, no. 39, pp. 4154–4156, 2013.

[25] F. Arith, S. A. M. Anis, M. M. Said, and C. M. I. Idris, "Low cost electro-deposition of cuprous oxide P-N homo-junction solar cell," *Advanced Materials Research*, vol. 827, pp. 38–43, 2014.

[26] M. A. Azhari, F. Arith, F. Ali, S. Rodzi, and K. Karim, "Fabrication of low cost sensitized solar cell using natural plant pigment dyes," *ARPN Journal of Engineering and Applied Sciences*, vol. 10, no. 16, pp. 7092–7096, 2015.

[27] Y. Lv, Y. Guo, H. Zhang, X. Zhou, and H. Chen, "Enhanced efficiency and stability of fully air-processed TiO_2 nanorods array based perovskite solar cell using commercial available CuSCN and carbon," *Solar Energy*, vol. 173, no. May, pp. 7–16, 2018.

[28] N. Arora, M. I. Dar, A. Hinderhofer, N. Pellet, F. Schreiber, S. M. Zakeeruddin, and M. Grätzel, "Perovskite solar cells with CuSCN hole extraction layers yield stabilized efficiencies greater than 20%," *Science*, vol. 358, no. 6364, pp. 768–771, 2017.

[29] J. W. Jung, C. C. Chueh, and A. K. Y. Jen, "High-Performance Semitransparent Perovskite Solar Cells with 10% Power Conversion Efficiency and 25% Average Visible Transmittance Based on Transparent CuSCN as the Hole-Transporting Material," *Advanced Energy Materials*, vol. 5, no. 17, pp. 1–7, 2015.

[30] A. Eldin, and A. Ali, "Effect of Dust Decompisition on Performance of Thin Film Photovoltaic Module in Harsh

Humid Climate," *Journal of Chemical Information and Modeling*, vol. 53, no. 9, pp. 1689–1699, 2013.

[31] N. D. Sankir, E. Aydin, and E. Ugur, "Spray pyrolized copper indium gallium sulfide abosrober layers for thin film solar cells," *Proceedings of 2013 International Conference on Renewable Energy Research and Applications, ICRERA 2013*, no. October, pp. 559–561, 2013.

[32] F. Matebese, R. Taziwa, and D. Mutukwa, "Progress on the synthesis and application of CuSCN inorganic hole transport material in perovskite solar cells," *Materials*, vol. 11, no. 12, 2018.

[33] A. Nizamuddin, F. Arith, I. J. Rong, M. Zaimi, A. S. Rahimi, and S. Saat, "Investigation of Copper(I) Thiocyanate (CuSCN) as a Hole Transporting Layer for Perovskite Solar Cells Application," *Journal of Advanced Research in Fluid Mechanics and Thermal Sciences*, vol. 78, no. 2, pp. 153–159, 2021.

[34] M. Kim, S. Park, J. Jeong, D. Shin, J. Kim, S. H. Ryu, K. S. Kim, Y. Yi, and H. Lee, "Band-Tail Transport of CuSCN: Origin of Hole Extraction Enhancement in Organic Photovoltaics," *Journal of Physical Chemistry Letters*, vol. 7, no. 14, pp. 2856–2861, 2016.

[35] I. S. Yang, M. R. Sohn, S. D. Sung, Y. J. Kim, Y. Yoo, J. Kim, and W. I. Lee, "Formation of pristine CuSCN layer by spray deposition method for efficient perovskite solar cell with extended stability," *Nano Energy*, vol. 32, pp. 414–421, 2017.

[36] G. A. Sepalage, S. Meyer, A. R. Pascoe, A. D. Scully, U. Bach, Y. Cheng, and L. Spiccia, "A facile deposition method for CuSCN: Exploring the influence of CuSCN on J-V hysteresis in planar perovskite solar cells," *Nano Energy*, vol. 32, pp. 310–319, 2017.

[37] D. Aldakov, C. Chappaz-Gillot, R.Salazar, V. Delaye, K. A. Welsby, V. Ivanova, and P.R. Dunstan, "Properties of electrodeposited CuSCN 2D layers and nanowires influenced by their mixed domain structure," *Journal of Physical Chemistry C*, vol. 118, no. 29, pp. 16095–16103, 2014.

[38] P. Pattanasattayavong, V. Promarak, and T. D. Anthopoulos, "Electronic Properties of Copper(I) Thiocyanate (CuSCN)," *Advanced Electronic Materials*, vol. 3, no. 3, pp. 1–33, 2017.

[39] J. Henry, P. Prema, D. P. Padiyan, K. Mohanraj, and G. Sivakumar, "Shape-dependent optoelectrical investigation of Cu 2+x Cd 1-x SnS 4 thin films for solar cell applications," *New Journal of Chemistry*, vol. 40, no. 3, pp. 2609–2618, 2016.

[40] B. Wang, Z. Zhanga, S. Yeb, L. Gaoa, T. Yana, Z. Bianb, C. Huang, and Y. Li, "Solution-Processable Cathode Buffer Layer for High-Performance ITO/CuSCN-based Planar Heterojunction Perovskite Solar Cell," *Electrochimica Acta*, vol. 218, pp. 263–270, 2016.

[41] P. M. Sirimanne and J. B. Zhang, "Characterization of electrochemically prepared CuSCN films and their capabilities of application in dye sensitized photovoltaic cells," *Sri Lankan Journal of Physics*, vol. 9, 2010.

[42] N. Wijeyasinghe and T. D. Anthopoulos, "Copper (I) thiocyanate (CuSCN) as a hole-transport material for large-area opto / electronics," vol. 104002, pp. 1–45, 2015.

[43] S. Z. Haider, H. Anwar, Y. Jamil, and M. Shahid, "A comparative study of interface engineering with different hole transport materials for high-performance perovskite solar cells," *Journal of Physics and Chemistry of Solids*, vol. 136, no. July 2019, p. 109147, 2020.

[44] B. N. Ezealigo, A. C. Nwanya, A. Simo, R. Bucher, R. U. Osuji, Malik Maaza, and M.V. Reddy, "A study on solution deposited CuSCN thin films: Structural, electrochemical, optical properties," *Arabian Journal of Chemistry*, vol. 13, no. 1, pp. 346–356, 2020.

[45] P. B. Ahirrao, S. R. Gosavi, and R. S. Patil, "Wide Band gap nanocrystalline CuSCN thin films deposited by modified chemical method," *Scholars Research Library,* no. 2 (3), pp. 29-33, 2011.

[46] X. Gao, X. Li, W. Yu, J. Qiu, and X. Gan, "Room-temperature deposition of nanocrystalline CuSCN fi lm by the modified successive ionic layer adsorption and reaction method," *Thin Solid Films*, vol. 517, no. 2, pp. 554–559, 2008.

[47] T. Prakash, S. Ramasamy, and B. S. Murty, "Effect of DC bias on electrical conductivity of nanocrystalline α-CuSCN," *AIP Advances*, vol. 1, no. 2, 2011.

[48] S. H. Meriam Suhaimy, N. Ghazali, F. Arith, and B. Fauzi, "Enhanced simazine herbicide degradation by optimized fluoride concentrations in TiO2 nanotubes growth," *Optik,* vol. 212, no. February, p. 164651, 2020..